JNC TN9400 2004－004

Feasibility Study on Long-Life Pb-Bi Cooled Reactor Capable to Follow the Load without Operation of Reactor Control System

（Research Document）

March, 2004

O-ARAI ENGINEERING CENTER

JAPAN NUCLEAR CYCLE DEVELOPMENT INSTITUTE

JNC TN9400 2004-004
March, 2004

Feasibility Study on Long-Life Pb-Bi Cooled Reactor Capable to Follow the Load without Operation of Reactor Control System

(Research Document)

TOSHINSKY Vladimir*

ABSTRACT

This report is devoted to feasibility study on long-life lead-bismuth cooled reactor capable to follow the load without operation of reactor control system (i.e., due to reactivity feedbacks only). The objective of research is to develop simple and economically competitive reactor design, in which the simplicity is improved by excluding of necessity for daily manipulation with control rods.

At the beginning of the study, the design of small Pb-Bi cooled reactor, developed at Tokyo Institute of Technology, was taken as a reference. For that design the load following capability by feedbacks has been confirmed. Additionally, the innovation for the reference design has been proposed in order to enhance such the capability. The point of innovation is strengthening of negative reactivity feedback by introduction of heat source (in the form of short fuel pins) at the bottom of radial lead-bismuth reflector. Implementation of the heat source allows controlling radial leakage during load change. In the case of small reactor the radial leakage plays essential role in neutron balance and, thus, utilization of heat source is effective.

As the next step, the optimization of reference design was performed to make it more simple (by keeping the same fuel pitch for all core), economically competitive (by increase of burnup), and more precisely estimated from neutronics viewpoint. The load following capability has then been confirmed for optimized design.

* JNC Post-doctoral researcher (01/04/2001 – 31/03/2004)
Fuel and Core System Engineering Group, System Engineering Technology Division, O-arai Engineering Center, JNC, Japan.

In order to fulfill the research targets, the followings analytical tools have been developed by the author during the study:

- **SAOS** (**S**imulated **A**nnealing Based **O**ptimization **S**ystem), which automatically performs design optimization with respect to reactivity swing or fuel burnup by stochastic manipulation of decision variables set, while satisfying design constrains.
- **EXPERT**, which automatically performs evaluation of design with pre-selected analytical approximation and generates all data necessary for the transient analysis (delay neutron data, reactivity maps);
- **SPAKS** (**S**implified **P**lant **A**nalysis **K**inetic **S**imulator), which calculates transient, such as load following. It also has capabilities for ATWS simulation.

All this systems will be described in the present report.

KEY WORDS: small reactor, long life core, Pb-Bi coolant, load-following

CONTENTS

LIST OF TABLES

LIST OF FIGURES

1. INTRODUCTION

1.1. Advantages of long-life cores

Designing of long-life core, which is one of objective of present study, have significance from the followings viewpoints.

First of all, this is improvement of economical performance. Elongation of core lifetime results in reduction of fuel fabrication costs leading to improvement of competitive ability of nuclear power plant as compare to ones operating using organic fuel. Achievement of high fuel burnup reduces the cost associated with refueling, storage of spent fuel, and its reprocessing being normalized to unit of produced power.

Secondly, this is the reduction of risk of unauthorized proliferation of fissile materials, since during long non-refueling reactor operation the plutonium, contained in fuel, is practically inaccessible for theft. This is especially important in the case of developing countries, where political instability may occur.

Thirdly, the long-life fast reactor effectively burns minor actinides and their concentration rather quickly goes to steady-state value. That result in reduction of specific fuel radiotoxicity as a function of energy produced, decreasing potential risk for the environment.

1.2. Benefits of Pb-Bi for designing compact plants

Utilization of heavy metal coolant – Pb-Bi eutectic alloy brings several important benefits to the reactor from both safety and economic viewpoints. This is basically provided by such properties of that coolant as chemical inertness and high boiling point, which forwards a reactor into “inherently safe” category. In Pb-Bi cooled reactor LOCA type accidents are deterministically excluded, because of low pressure in the reactor. The same is true for the chemical explosions and fire. For that reason there is no necessity for safety systems designed to reduce probability or alleviate consequences of such accidents in the case the water or sodium cooled reactors. This make nuclear power plant simpler and reduces the costs for construction and operation.

Additionally, solidification of the coolant at temperature 125 ^{o}C makes possible safe transportation of the fueled reactor (safe from nuclear and radiation viewpoints) with “frozen” coolant. That also reduces the risk of unauthorized proliferation during transportation.

1.3. Profits from capability to follow the load without operation of reactor control system

Important feature, which improves the safety and simplify reactor operation, is its capability to change the power according to change of electric load (load following) without operation of reactor control system. Combination of feedbacks allows excluding reactivity margin reserved for the power control and, thus, possibility of accident in the case of its incidental release.

Reactor control system becomes simpler, since automatic power controller is excluded. That improves reliability of reactor, since its operation would not be affected neither possible failure of automatic power controller or operator’s mistake.

1.4. Brief overview of present study

At the beginning of the study, the design of small Pb-Bi cooled reactor, developed at Tokyo Institute of Technology, was taken as a reference. For that design the load following capability by feedbacks has been confirmed.

Additionally, the innovation for the reference design has been proposed in order to enhance such the capability. The point of innovation is strengthening of negative reactivity feedback by introduction of heat source (in the form of short fuel pins) at the bottom of radial lead-bismuth reflector. Implementation of the heat source allows controlling radial leakage during load change. In the case of small reactor the radial leakage plays essential role in neutron balance and, thus, utilization of heat source is effective.

At the initial stage, research was performed using simple computational models from neutronics viewpoint (RZ, Diffusion approximation). In order to make the analysis accurate with reasonable requirement on computation costs, several computational approximations were implemented and the best suited for this particular problem had been selected (3D, Diffusion, 18 gr. - for the fuel and structure density reactivity feedbacks; 3D, Transport, 18 gr. – for the coolant density feedbacks).

As the final step of the research, the optimization of reference design have been performed with the purpose to make it simpler by keeping the same fuel pin pitch for all core and economically competitive by increase of fuel burnup. The load following capability has been then confirmed for optimized design.

2. PRELIMINARY INVESTIGATION OF LOAD FOLLOWING CAPABILITY FOR TYPICAL SMALL SIZE LONG-LIFE PB-BI COOLED REACTOR

2.1. Description of calculation system SPAKS and load change simulation model

For simulation of load-following operation the system **SPAKS** (**S**implified **P**lant **A**nalysis **K**inetic **S**imulator) have been developed, which models kinetic behavior of primary circuit: core, hot/cool pools by solving time-dependent equations for mass, momentum, and energy conservation /1/. For primary and secondary sides of SG, the steady-state equations for mass, momentum, and energy conservation are repeated at each time-step during transient (quasistatic approach). For power computation, the point kinetic approximation is used. Multi-channel core model is applied for reactivity computations.

The simulation of the secondary circuit is limited by SG only. During power manoeuvrings, the pressure in the secondary loop assumed to be constant. The secondary flow rate is assumed to be proportional to load and SG inlet specific enthalpy of water is kept constant during the transient. The model for load following simulation is shown on Figure 1 and is taken from the Reference 2.

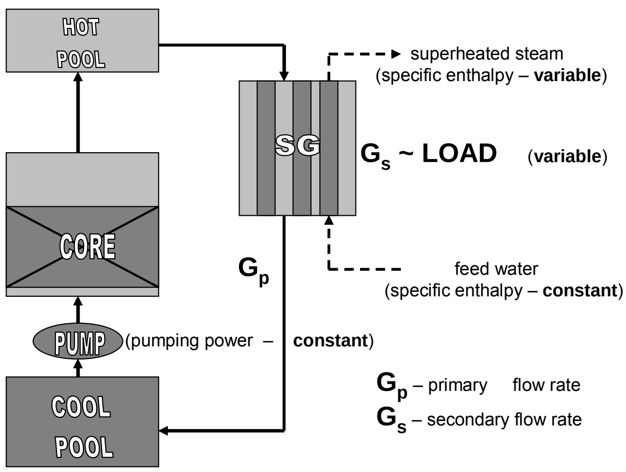

Fig 1. Load following simulation model

2.2. Description of reference design

2.2.1. Specifications of reference design

The Figure 2 and 3 shows layout of reference core and core axial cross section, Tables1 and 2 demonstrate the reference core specifications and S/A specifications, respectively. The core has inner blanket region and axial enrichment heterogeneity in the inner core region. The pitch of fuel in the inner blanket region is decreased to reduce the positive void and coolant density effect and the axial heterogeneity is purposed to obtain small burnup reactivity swings.

Table 1. Reference design parameters.

Parameter	Value
Thermal output, MWt	150
Core lifetime, years	15
Core equivalent diameter, cm	194.97
Core fuel column length, cm	130.0
Low enrichment zone height, cm	78.0
Top/ Bottom shielding thickness, cm	22.5 / 65.0
Fuel material	(Pu,U) ^{15}N
Clad material	ODS
Wrapper material	PNC-FMS
Coolant material	Pb-Bi eutectic
Bonding material	Pb-Bi eutectic
Core support plate	316FR
CRD line	PNC-FMS
Above core load pads	PNC-FMS
Total number of assemblies	169
S/A pitch, mm	237.73
Number of (core+blanket) assemblies	51+6
Number of reflector assembles	30
Number of shielding assemblies	78
Number of CR assemblies	4
Primary condition (inlet/outlet), C	360/510
Temperature rise	150
Total flow rate, kg/s	6830

The concept of such the core configuration is taken from Reference 3, where the effect of axial and radial enrichment heterogeneities on achieving small burnup reactivity swings has been analyzed. In that paper the investigation was, however, limited by RZ diffusion calculation model, without any considerations about control rods. Later on, more detailed analysis of core and plant design have been done in Reference 4, where the concept was named LSPR (**L**ead–Bismuth Eutectic Cooled **L**ong-**L**ife **S**afe **S**imple **S**mall **P**ortable **P**roliferation **R**esistant **R**eactor).

Table 2. Reference fuel subassembly specifications.

Parameter	Value
Pin diameter, mm	14 .970
Cladding thickness, mm	0.800
Pellet diameter, mm	11.960
Pellet cladding gap, mm	0.705
Pin pitch (blanket *), mm	17.470 (15.560 *)
Pin gap (blanket *), mm	2.470 (0.560 *)
Pitch/diameter ratio (blanket *)	1.165 (1.037 *)
Total number of fuel pins	9921
S/A size (flat-to-flat), mm	235.73
S/A wall thickness, mm	2.0
Number of fuel pins per S/A (blanket *)	169 (217 *)
Porosity per ring (blanket *)	4.4070 (1.0366 *)
Fuel smeared density, % TD	80
Fuel pellet density, % TD	100
Gas plenum length, cm	70.0
CDF (EOC)	(not estimated)
Fuel pin bundle spacing	Grid spacers

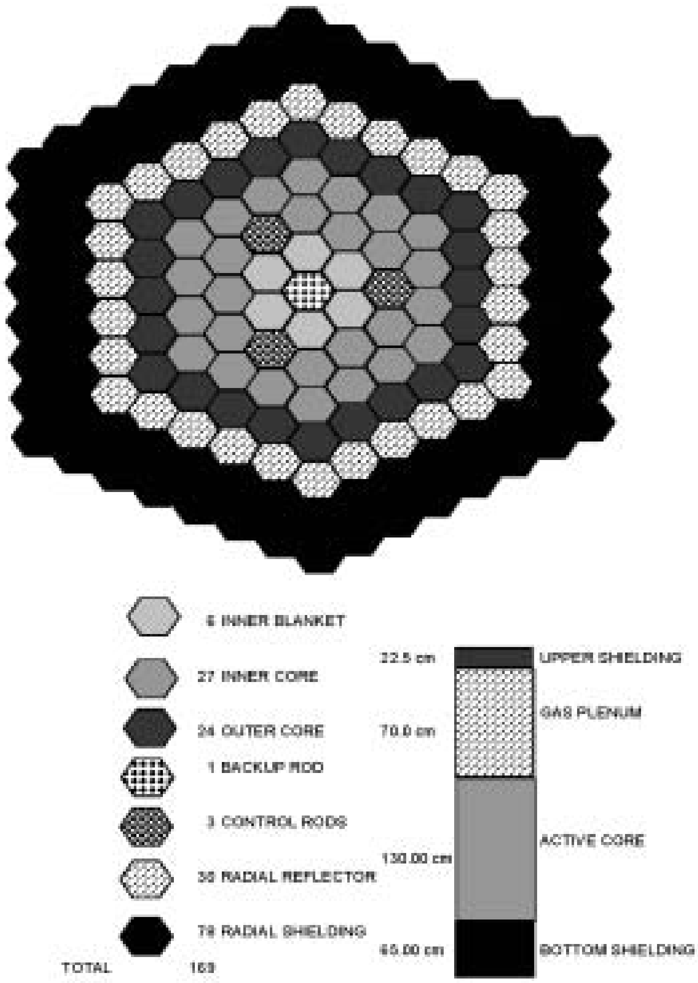

Fig 2. Layout of reference core and subassembly axial profile.

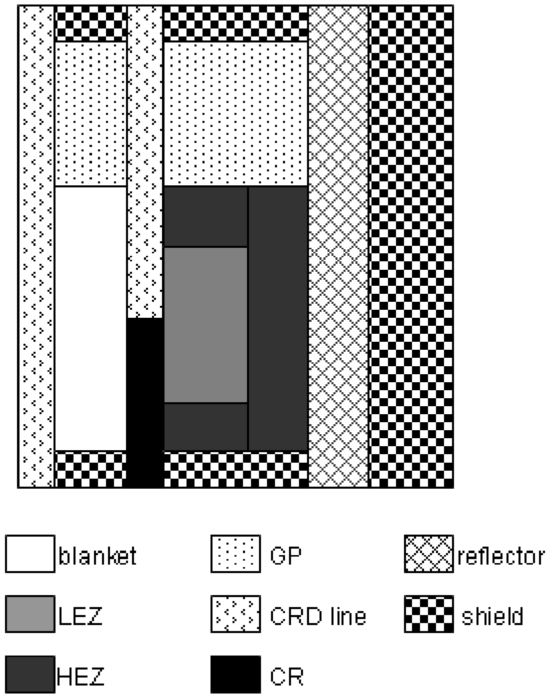

Fig 3. Reference core axial cross section.

2.2.2. Description of evaluation system – EXPERT

To simulate reactor kinetics during load change transient is necessary to compute delayed neutron data and reactivity coefficients. Since the leakage plays important role for the small reactor, it is precise treatment that is important for computation of reactivity coefficients and core performance evaluation. For the purpose to find appropriate approximation the system **EXPERT** was developed, which consists of set of batch files & utility programs automatically generating INPUTs for set of computer codes, which allows calculation of reactivity coefficients and evaluation of core performance in different approximations. The **EXPERT** system consists of two parts: first part - generation of effective microscopic cross-sections (see Figure 4) and design evaluation part (see Figure 5). More specifically, the system operates as followings:

- for pre-selected required neutronics approximation and given initial guess of temperatures it performs iterative burnup & thermal computations, updating microscopic cross-sections until convergence of temperatures at MOC;
- using obtained micro cross-section set, performs burnup calculation from BOC to EOC, evaluating burnup reactivity swings and providing number densities for MOC and EOC;

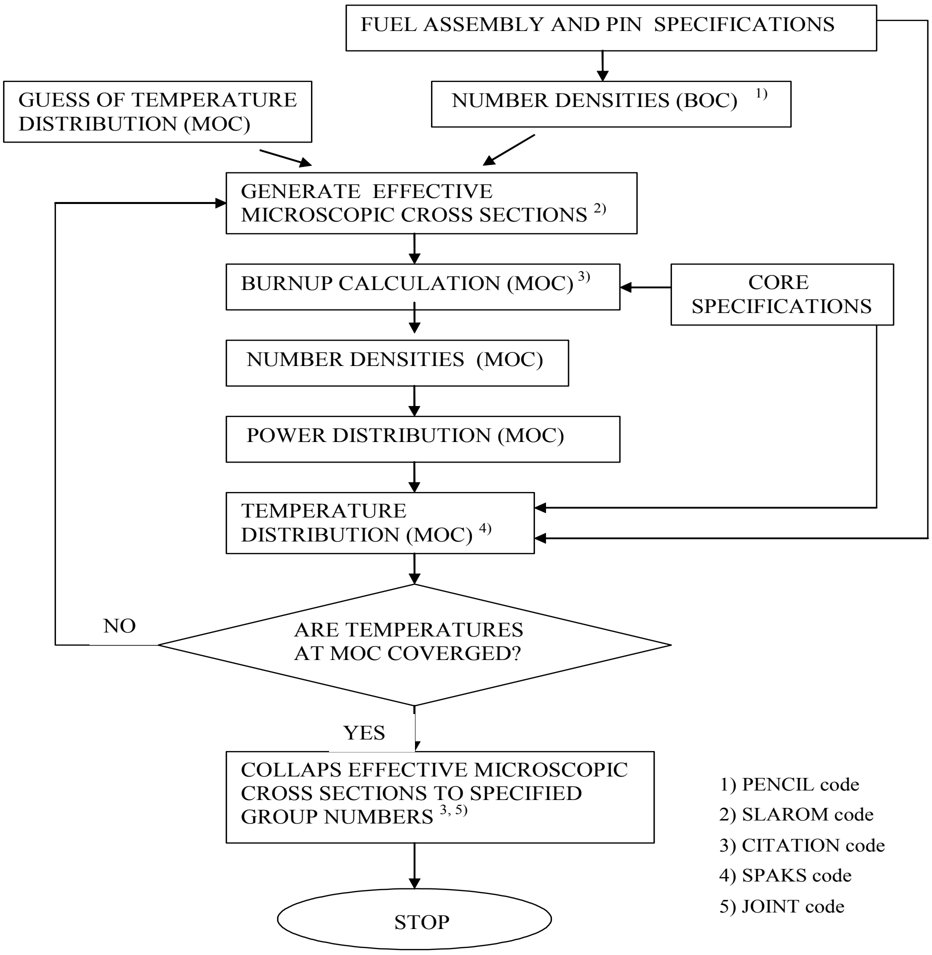

Fig 4 EXPERT (PART I) Generation of effective microscopic cross section set.

- using calculated number densities, the system generates micro-cross sections sets for BOC/MOC/EOC, generate delayed neutrons data/reactivity maps/ temperatures for BOC/MOC/EOC and required core characteristics for BOC/MOC/EOC.

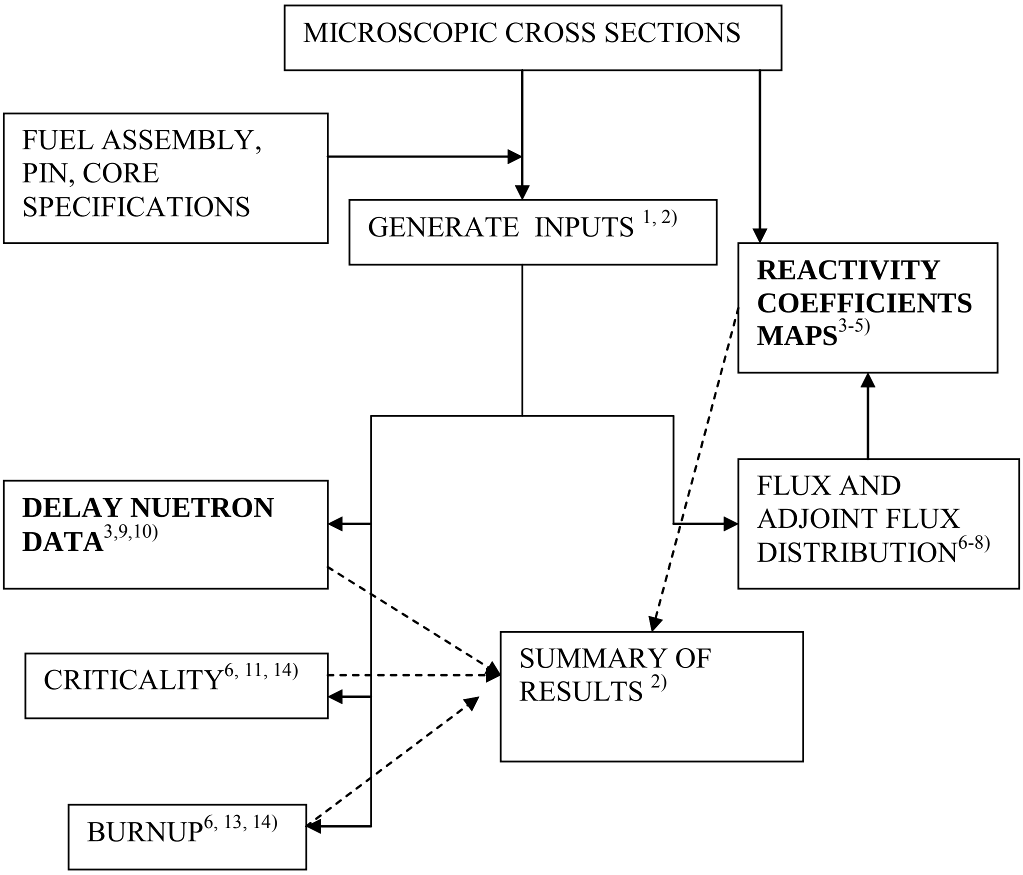

1) JOINT code
2) UTILITY programs
3) PERKY code
4) SNPERT code
5) SNPET3D code
6) CITATION code
7) TWOTRAN code
8) TRITAC code
9) CITBETA code
10) SRAC system
11) TRITAC code
12) NSHEX code
13) NSHEX_BURN code
14) MOSES code

Figure 5. EXPERT (PART II) Design evaluation.

2.2.3. Schematics of neutronics and thermal hydraulics calculation model.

As it seen from the Figure 6, the model assumes 7 channels (from core center to periphery): channel for backup rod, inner blanket, primary control rod, enrichment zone with axial heterogeneity, high enrichment zone, radial reflector and radial shield. For temperature computations, the power density averaged over fuel SAs belonging to corresponding channel was used. Mass flow rate through channels 1, 3, 6 was set up – 0.1% rel. and through channel 7 – 5% /2/.

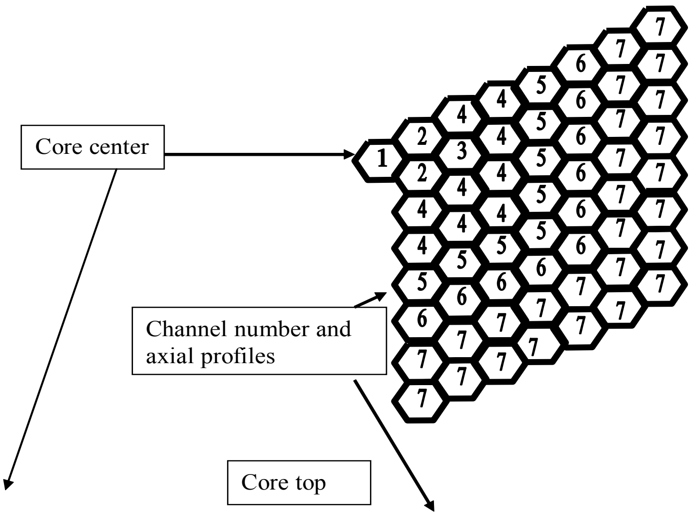

Core top

Ch 1	Ch 2	Ch 3	Ch 4	Ch 5	Ch 6	Ch 7
CRDV	SHD_T	CR	SHD_T	SHD_T	REF	SHD_R
CRDV	GSPL	CR	GSPL	GSPL	REF	SHD_R
CRDV	IBL	CR	HEZ	HEZ	REF	SHD_R
CRDV	IBL	CR	LEZ	HEZ	REF	SHD_R
CRDV	IBL	CR	LEZ	HEZ	REF	SHD_R
CRDV	IBL	CRDV	LEZ	HEZ	REF	SHD_R
CRDV	IBL	CRDV	LEZ	HEZ	REF	SHD_R
CRDV	IBL	CRDV	HEZ	HEZ	REF	SHD_R
CRDV	SHD_B	CRDV	SHD_B	SHD_B	REF	SHD_R

Core bottom

CRDV: Drives of control rods [Channel - **3**] and backup rod [Channel - **1**]

SHD_B: Bottom shield

GSPL: Gas plenum

CR: Control rod

SHD_T: Top shielding

REF: Radial reflector

SHD_R: Radial shield

IBL: Inner blanket

LEZ: Low enrichment zone

HEZ: High enrichment zone

Fig 6. Model for spatial reactivity coefficients and thermal hydraulics calculation

2.2.4. Calculation of reactivity coefficients and core performance for reference design

The details of finding appropriate approximation are described in Reference 5, where the following conclusions had been made:

- 3D (HexZ), 18GR, diffusion approximation is appropriate for computation of all coefficients, excluding coolant density feedback;
- 3D (XYZ), 18 GR, transport approximation for coolant density feedbacks.

Core characteristics, given by Table 3, are evaluated using diffusion HexZ 18 GR approximation. Reactivity coefficients, calculated in above approximations, are represented by Tables 4 – 7.

Table 3. Reference core performance.

Parameter		Value
Average linear power rating , W/cm		116.3
Maximum linear power rating, W/cm	[EOC]	214.2
Peak power factor	[EOC]	1.769
Conversion ratio	[MOC]	1.185
Peak fast neutron dose (E > 0.1 MeV) n/cm2		2.49e+23
Pu Enrichment (inner/outer core), %		12.7900/ 13.7800
Burnup reactivity swings, dk/(kk')%		0.19
HM inventory, kg		19482.18
Average burnup , GWd/t		43.17
Peak burnup , GWd/t		79.52
Void (core region), dk/(kk')%, [$]		2.107E-2, [6.03]

Table 4. Reactivity coefficients distribution (Doppler) (Ref. core)

Ch 1	Ch 2	Ch 3	Ch 4	Ch 5	Ch 6	Ch 7
0.000E+00	0.000E+00	0.000E+00	0.000E+00	0.000E+00	0.000E+00	0.000E+00
0.000E+00	0.000E+00	0.000E+00	0.000E+00	0.000E+00	0.000E+00	0.000E+00
0.000E+00	-6.963E-05	0.000E+00	-2.392E-04	-2.291E-04	0.000E+00	0.000E+00
0.000E+00	-3.143E-05	0.000E+00	-1.170E-04	-1.156E-04	0.000E+00	0.000E+00
0.000E+00	-2.928E-05	0.000E+00	-1.190E-04	-1.216E-04	0.000E+00	0.000E+00
0.000E+00	-2.238E-05	0.000E+00	-1.098E-04	-1.160E-04	0.000E+00	0.000E+00
0.000E+00	-1.486E-05	0.000E+00	-9.253E-05	-9.975E-05	0.000E+00	0.000E+00
0.000E+00	-1.346E-05	0.000E+00	-1.237E-04	-1.372E-04	0.000E+00	0.000E+00
0.000E+00	0.000E+00	0.000E+00	0.000E+00	0.000E+00	0.000E+00	0.000E+00
TOTAL CORE		dK/KK'	: -1.801E-03			

Table 5. Reactivity coefficients distribution (fuel density) (Ref. core)

Ch 1	Ch 2	Ch 3	Ch 4	Ch 5	Ch 6	Ch 7
0.000E+00	0.000E+00	0.000E+00	0.000E+00	0.000E+00	0.000E+00	0.000E+00
0.000E+00	0.000E+00	0.000E+00	0.000E+00	0.000E+00	0.000E+00	0.000E+00
0.000E+00	-7.573E-04	0.000E+00	4.314E-02	4.051E-02	0.000E+00	0.000E+00
0.000E+00	-9.369E-05	0.000E+00	2.150E-02	2.214E-02	0.000E+00	0.000E+00
0.000E+00	-1.107E-04	0.000E+00	2.174E-02	2.290E-02	0.000E+00	0.000E+00
0.000E+00	-1.333E-04	0.000E+00	1.962E-02	2.109E-02	0.000E+00	0.000E+00
0.000E+00	-5.634E-05	0.000E+00	1.583E-02	1.729E-02	0.000E+00	0.000E+00
0.000E+00	-2.367E-05	0.000E+00	2.243E-02	2.347E-02	0.000E+00	0.000E+00
0.000E+00	0.000E+00	0.000E+00	0.000E+00	0.000E+00	0.000E+00	0.000E+00
TOTAL CORE		(dK/KK')/(dρ/ρ): 2.905E-01				

Table 6. Reactivity coefficients distribution (structure density) (Ref. core)

Ch 1	Ch 2	Ch 3	Ch 4	Ch 5	Ch 6	Ch 7
0.000E+00	0.000E+00	0.000E+00	0.000E+00	0.000E+00	0.000E+00	0.000E+00
0.000E+00	0.000E+00	0.000E+00	0.000E+00	0.000E+00	0.000E+00	0.000E+00
0.000E+00	-5.369E-04	0.000E+00	-5.520E-03	-3.876E-03	0.000E+00	0.000E+00
0.000E+00	-2.588E-04	0.000E+00	-3.787E-03	-2.814E-03	0.000E+00	0.000E+00
0.000E+00	-2.115E-04	0.000E+00	-3.775E-03	-2.957E-03	0.000E+00	0.000E+00
0.000E+00	-1.154E-04	0.000E+00	-3.201E-03	-2.669E-03	0.000E+00	0.000E+00
0.000E+00	-3.551E-05	0.000E+00	-2.355E-03	-2.050E-03	0.000E+00	0.000E+00
0.000E+00	3.265E-05	0.000E+00	-1.816E-03	-1.586E-03	0.000E+00	0.000E+00
0.000E+00	0.000E+00	0.000E+00	0.000E+00	0.000E+00	0.000E+00	0.000E+00
TOTAL CORE		(dK/KK')/(dρ/ρ):	-3.75E-02			

Table 7. Reactivity coefficients distribution (coolant density) (Ref. core)

Ch 1	Ch 2	Ch 3	Ch 4	Ch 5	Ch 6	Ch 7
0.000E+00	0.000E+00	0.000E+00	0.000E+00	0 .000E+00	0.000E+00	0.000E+00
0.000E+00	<u>9.109E-05</u>	0.000E+00	<u>3.241E-03</u>	<u>5.456E-03</u>	**2.381E-03**	0.000E+00
0.000E+00	-7.103E-05	0.000E+00	-3.669E-03	-1.263E-03	**1.046E-02**	0.000E+00
0.000E+00	-2.664E-05	0.000E+00	-3.385E-03	-1.847E-03	**5.003E-03**	0.000E+00
0.000E+00	5.012E-06	0.000E+00	-3.312E-03	-1.977E-03	**4.299E-03**	0.000E+00
0.000E+00	5.620E-05	0.000E+00	-2.642E-03	-1.733E-03	**3.182E-03**	0.000E+00
0.000E+00	8.495E-05	0.000E+00	-1.774E-03	-1.204E-03	**1.984E-03**	0.000E+00
0.000E+00	1.598E-04	0.000E+00	-1.309E-04	3.837E-04	**1.887E-03**	0.000E+00
0.000E+00	0.000E+00	0.000E+00	0.000E+00	0.000E+00	0.000E+00	0.000E+00
CORE		(dK/KK')/(dρ/ρ):	-2.23E-02			
GAS PLENUM		(dK/KK')/(dρ/ρ):	<u>8.79E-03</u>			
RADIAL REFLECTOR		(dK/KK')/(dρ/ρ)):	**2.920E-02**			

2.3. Verification of load following capability without operation of reactor control system for typical small size long-life Pb-Bi cooled reactor

2.3.1. Mathematical formulating of reactivity feedbacks

Using reactivity coefficients maps, the feedbacks are calculated by formulas represented by Figure 7 and data given by Table 9. Delayed neutron data are represented by Table 8. More specifically, two types of computer calculations are done to produce components of the thermal expansion effects on reactivity. One calculation type is PERKY calculation (exact perturbation theory). These calculate the reactivity effects of density changes in the fuel and structure materials (formulas 1.3, 1.5 of Figure 7, calculation results – Table 5, 6 of previous section). As mentioned above, effect of the coolant density change was calculated using SNPERT3D (transport approximation) (formula 1.4 of Figure 7, calculation results – Table 7 of previous section). The second type of calculations is MOSES (3D, HexZ, 18 GR) calculations for the core, but either axial or subassembly pitch slightly increase (say 1%), the number density remain

Table 8. Delayed neutron data (Ref. core)

Parameter	Value
Prompt neutron lifetime	2.60659E-7
Delay neutron fraction	3.49145E-3
$\beta 1$	7.35605E-5
$\beta 2$	7.53859E-4
$\beta 3$	6.47427E-4
$\beta 4$	1.30582E-3
$\beta 5$	5.90596E-4
$\beta 6$	2.20110E-4
$\lambda 1$	1.30203E-2
$\lambda 2$	3.13708E-2
$\lambda 3$	1.34392E-1
$\lambda 4$	3.45264E-1
$\lambda 5$	1.36693E+0
$\lambda 6$	3.72921E+0

the same. These calculate the reactivity effect of changes in core height and radial dimensions (formulas 1.1, 1.2 of Figure 7, calculation results – Table 9).

Formula 1.6 takes into account effect of fuel pin elongation when computing fuel density feedback component, and formulas 1.8 and 1.9 of Figure 7 takes into account effect of coolant exclusion due to steel expansion when calculating cladding and wrapper density change reactivity effect.

The formula 1.10, which calculates feedback due to control rod drive line elongation, takes also into account core axial expansion. The formalism was taken from the Reference 6.

Table 9. Supplement data for reactivity feedbacks computation.

Parameter		Value
K_R		2.253E-1
K_H		8.991E-2
Volume fractions:		
Fuel,	v_f	0.38782 (0.49797*)
Coolant ,	v_c	0.35916 (0.18657*)
Cladding,	v_{cl}	0.12297 (0.15789*)
Wrapper,	v_w	0.03309 (0.03309*)
Bonding (Pb-Bi),	v_b	0.09696 (0.12449*)
* blanket		
Linear expansion coefficients, dl/l/^{0}C		
Fuel,	α_f	9.839E-6
Cladding,	α_{cl}	1.212E-5
Coolant,	α_c	-1.190E-4
Wrapper,	α_w	1.222E-5
Support,	α_{sup}	1.778E-5
CR drive line,	α_{crd}	1.258E-5
Above core load pads,	α_{aclp}	1.258E-5

$$K_R = \frac{\Delta k / kk'}{\Delta R / R} \tag{1.1}$$

$$K_H = \frac{\Delta k / kk'}{\Delta H / H} \tag{1.2}$$

$$K_F = \frac{\Delta k / kk'}{\Delta \rho_F / \rho_F} \tag{1.3}$$

$$K_C = \frac{\Delta k / kk'}{\Delta \rho_c / \rho_c} \tag{1.4}$$

$$K_S = \frac{\Delta k / kk'}{\Delta \rho_s / \rho_s} \tag{1.5}$$

$$\Delta\rho_F = \alpha_f (K_H - K_F) \Delta T_f \tag{1.6}$$

$$\Delta\rho_C = \alpha_c K_c \Delta T_c \tag{1.7}$$

$$\Delta\rho_{CL} = -\alpha_{cl} \{ 2\frac{(V_f + V_b + V_{cl})}{(V_b + V_c)} K_c + \frac{(V_{cl})}{(V_{cl} + V_w)} K_s \} \Delta T_{cl} \tag{1.8}$$

$$\Delta\rho_W = -\alpha_w \{ 2\frac{(V_w)}{(V_b + V_c)} K_c + \frac{(V_w)}{(V_{cl} + V_w)} K_s \} \Delta T_w \tag{1.9}$$

$$\Delta\rho_{CRD} = W \left\{ -\alpha_{crd} L_{crd} \Delta T_{crd} + \alpha_f L_f \Delta T_f \right\} \tag{1.10}$$

$$\begin{aligned} \Delta\rho_{BOWING} = &\{ K_R - 2(K_F + K_s) - 2\frac{(V_b)}{(V_b + V_c)} K_c + 2\frac{(1 - V_c)}{(V_b + V_c)} K_c \} \times \\ &\{ \alpha_{sup} \Delta T_{sup} + \frac{H_c}{H_{aclp}} (\alpha_{aclp} \Delta T_{aclp} - \alpha_{sup} \Delta T_{sup}) \} \end{aligned} \tag{1.11}$$

where
k, k' *– normal and perturbated multiplication factors, respectively;*
R, H *– core height and radius, respectively;*
H_c, H_{aclp} *– dis tan ce from bottom of core sup port plate to core center and to above core load pads, respectively*
$V_{f,c,cl,w,b}$ *– volume fractions of fuel, coolant, cladding, wrapper, bonding, respectively*

$\alpha_{f,cl,w,sup,crd,aclp}$ *– liner exp ansion coefficients for fuel, cladding, wrapper, core sup port plate, control rod drive line, above core load pads, respectively*
α_c *– coolant density coefficient*
$L_{crd,f}$ *– CR drive line length and fuel column length, respectively;*
W *– local CR worth (cent / cm).*

Fig 7. Reactivity feedbacks formalism.

Core bowing model, given by Formula 1.11 of Figure 7 described in detail in Reference 2.

2.3.2. Simulation of load following without operation of reactor control system for typical small size long-life Pb-Bi cooled reactor

Reactor transient is simulated by SPAKS code, which is reactor power control by the change of feed water flow rate. Figures 8-11 shows the results for load following simulation, where feed water flow is decreased at rate of~ 2%/min. referring the commercial nuclear power plant. In this analysis, the effect of core bowing and radial expansion of core support structure are not taken into account, because its precise treatment is very complicated. The "trapezoidal" model (given by Equation 1.11 of Figure 7), which sometimes used for safety analysis is not considered, because it has large inaccuracies. Since EOC condition is considered, the CR is located at the core top, where its local worth is rather small. Thus, negative CR drive line elongation reactivity is almost negligible.

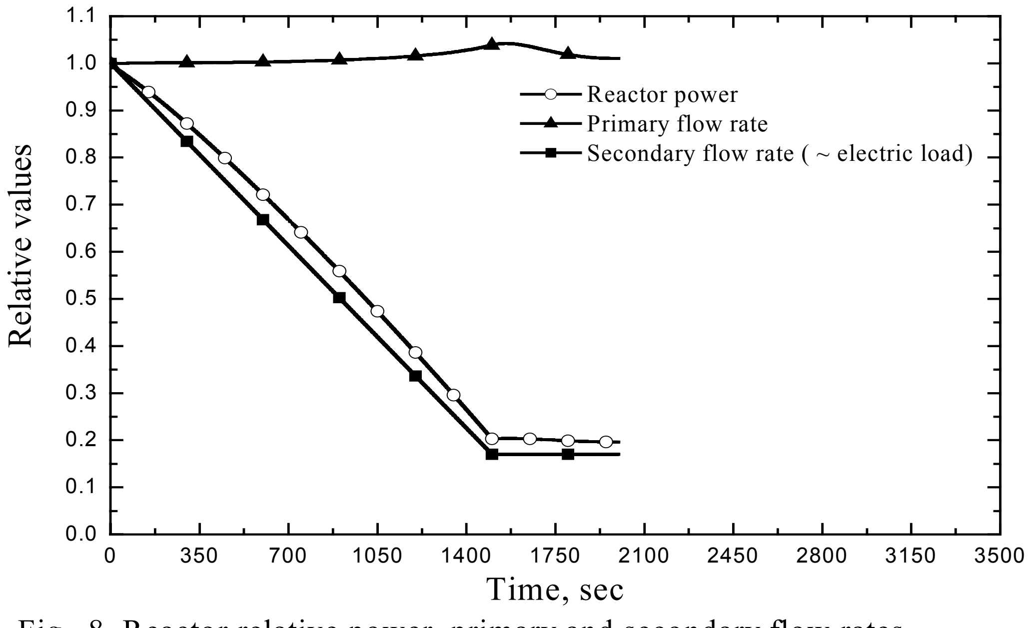

Fig. 8. Reactor relative power, primary and secondary flow rates.

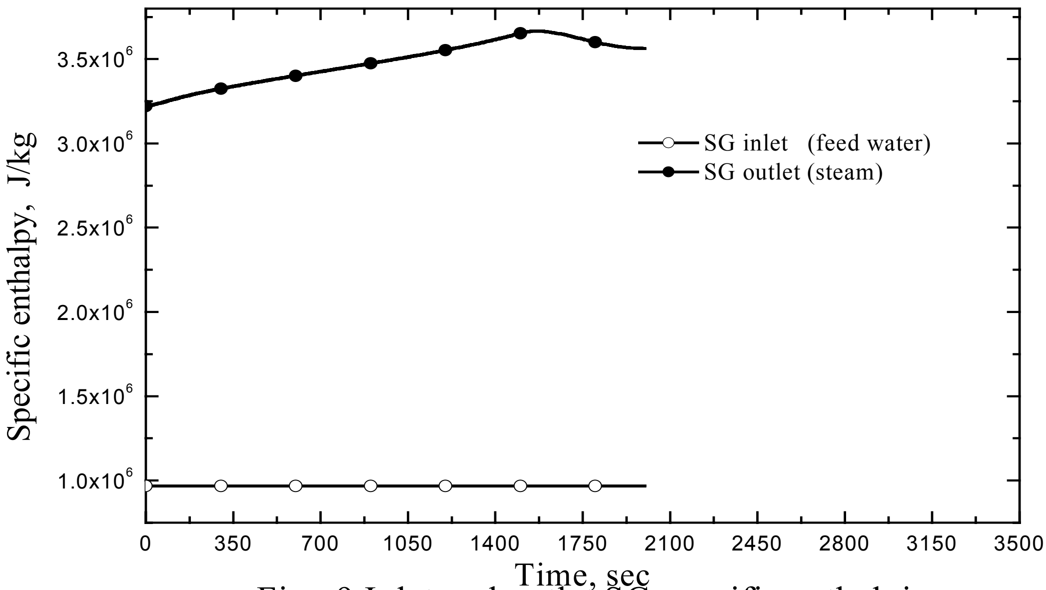

Fig. 9 Inlet and outlet SG specific enthalpies.

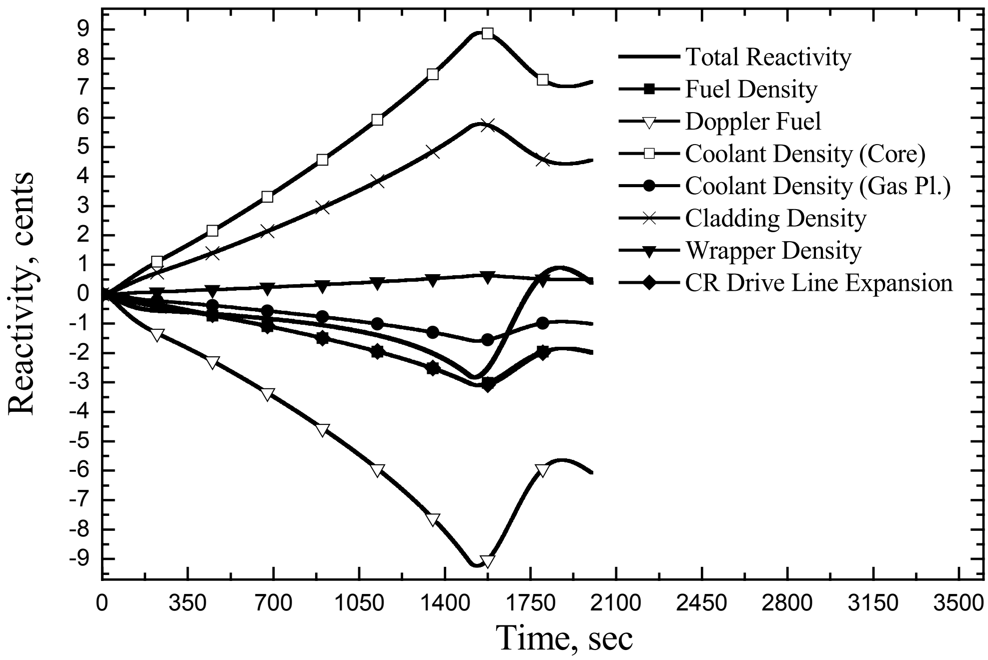

Fig. 10 Reactivity components.

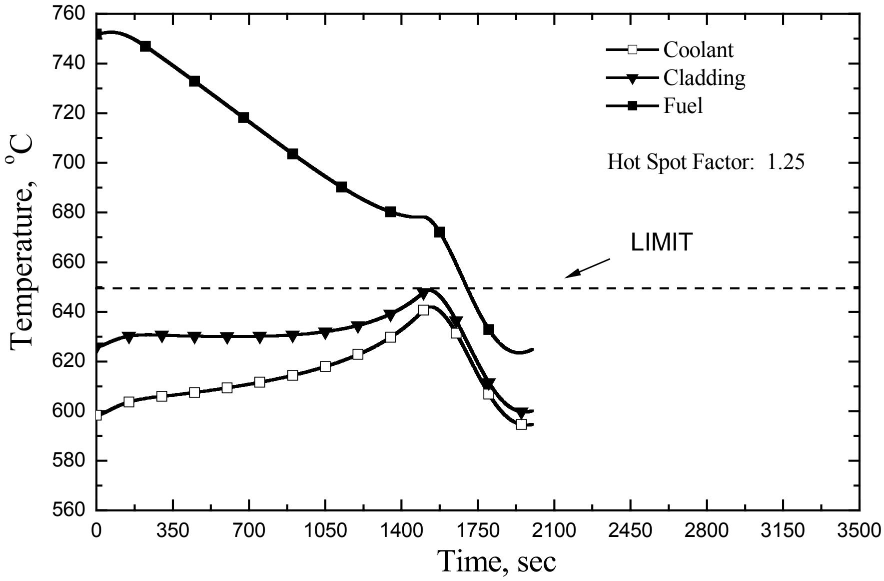

Fig. 11 Hot spot temperatures.

It is seen from the Figure 10 that the dominant negative feedback is Doppler, while positive – coolant and structure density. During the transient the cool pool temperature increases, since heat removal in SG decreases. In spite of power reduction, the average core outlet temperature and hot pool temperature increases. This is caused by the fact the increment of inlet temperature is greater than reduction of temperature rise in the core. The fuel density and CRD line expansion reactivity are almost coincides, since change in core average fuel temperature is very close to change in hot pool temperature.

Figure 11 illustrates that cladding hot spot temperature slightly increases during the transient, reaches the limit temperature from corrosion viewpoint (large hot spot factor 1.25 is used for the analysis conservativeness) and then decreases, when power reaches reduced steady-state value. It may be concluded that load following by feedbacks is feasible, since cladding hot spot temperature remains under limitation from corrosion viewpoint even with applying large hot spot factor. However, the tendency of cladding hot spot temperature increase during load reduction is not desirable feature.

2.3.3. Enhancement of load following capability without operation of reactor control system

In the case of Pb-Bi cooled reactors, the negative feedback can be strengthened by designing radial reflector not as stagnant region, but as the channel. That allows including effect of coolant density change in radial reflector region, which is negative with temperature increase. In the of small reactor this effect is strong, since radial leakage play important role in neutron balance. As it was mentioned in previous section, the temperature in cool pool increases during load reduction that will result in increase of temperature of coolant in radial reflector region, if its designed as a simple channel, and, thus, the negative feedback will be enhanced. Utilization of heat source (HS) in the form of short fuel pins in radial reflector channel, as schematically shown on Fig. 12, make the reactor design slightly complicated, but has benefit in the case of ULOF event /7/. In the case of HS implementation and adjustment of proper flow rate through radial reflector channel, the mentioned feedback is driving by temperature change similar to average core outlet temperature.

Results of calculation of load change transient, where feedback due to HS is taken into account, are shown on Fig. 13 and Fig. 14. As seen from the Fig. 13, the feedback due to HS is even more effective then feedback due to fuel density change. Fig. 14 demonstrates stable decrease of hot spot cladding temperature during the transient. Thus, when HS is implemented, load following without operation of reactor control system become feasible in the frame of considered simulation model.

It should be noted that for sodium cooled reactors, the radial reflector is usually made from steel and, thus, the mentioned feedback mechanism can not be realized in such the reactors.

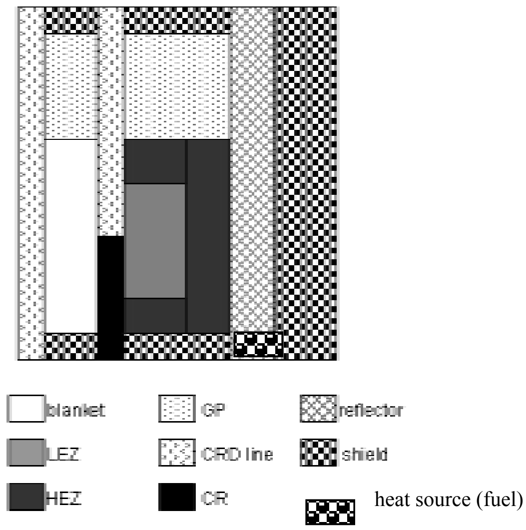

Fig 12. Utilization of heat source in radial reflector region.

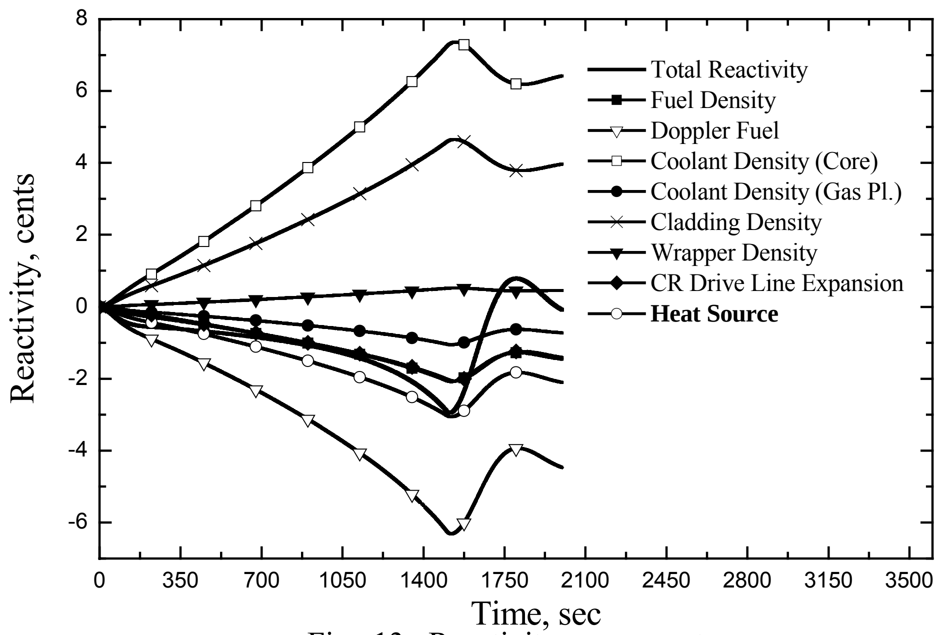

Fig. 13 Reactivity components.

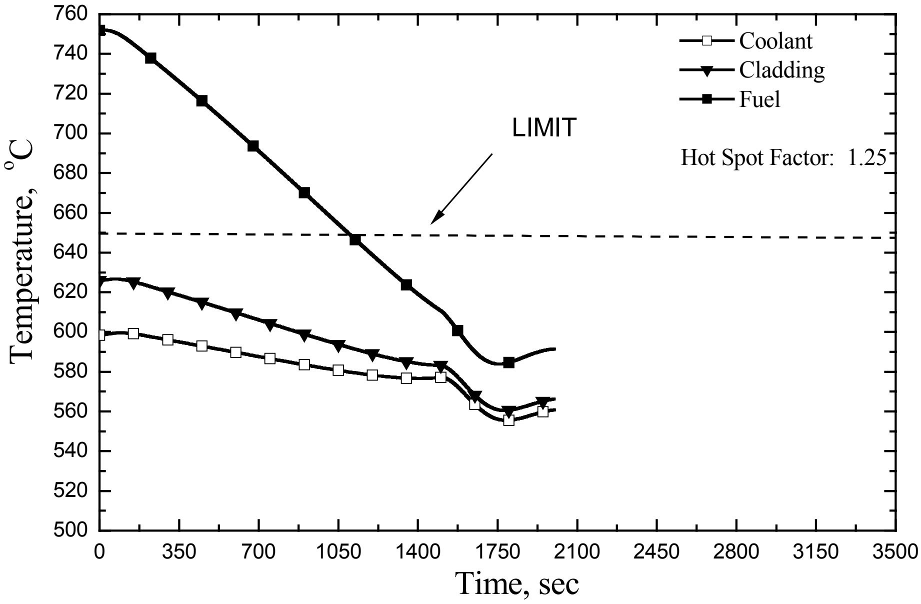

Fig. 14 Hot spot temperatures.

2.4. Reasons for optimization of reference design

The reasons for modification are the followings:

a. reference design has small discharged burnup (See Table 3);

b. different fuel pitch at the blanket and fuel regions makes design less attractive(See Table 2);

c. pin gap in blanket region is less than 1 mm that is usually considered as a constraint (See Table 2).

3. CORE DESIGN OPTIMIZATION

3.1. Optimization procedure

3.1.1. Design modifications

The following modifications have been applied to the reference design:

a. the pin pitch at blanket region is assigned same as in core region;

b. fuel smear density is increased from 80% to 84%, since burnup value is low and there is no necessity for large fuel-inner cladding gap;
c. operation cycle is increased from 15 to 30 years;
d. keep burnup reactivity swings same or smaller than for the case of reference design.

3.1.2. Description of optimization tool – SAOS

To obtain small reactivity swing by adjustment of enrichments and relative value of axial enrichment heterogeneity for inner core region the optimization system SAOS (See Figure 15), based on Simulated Annealing (SA) optimization method have been developed.

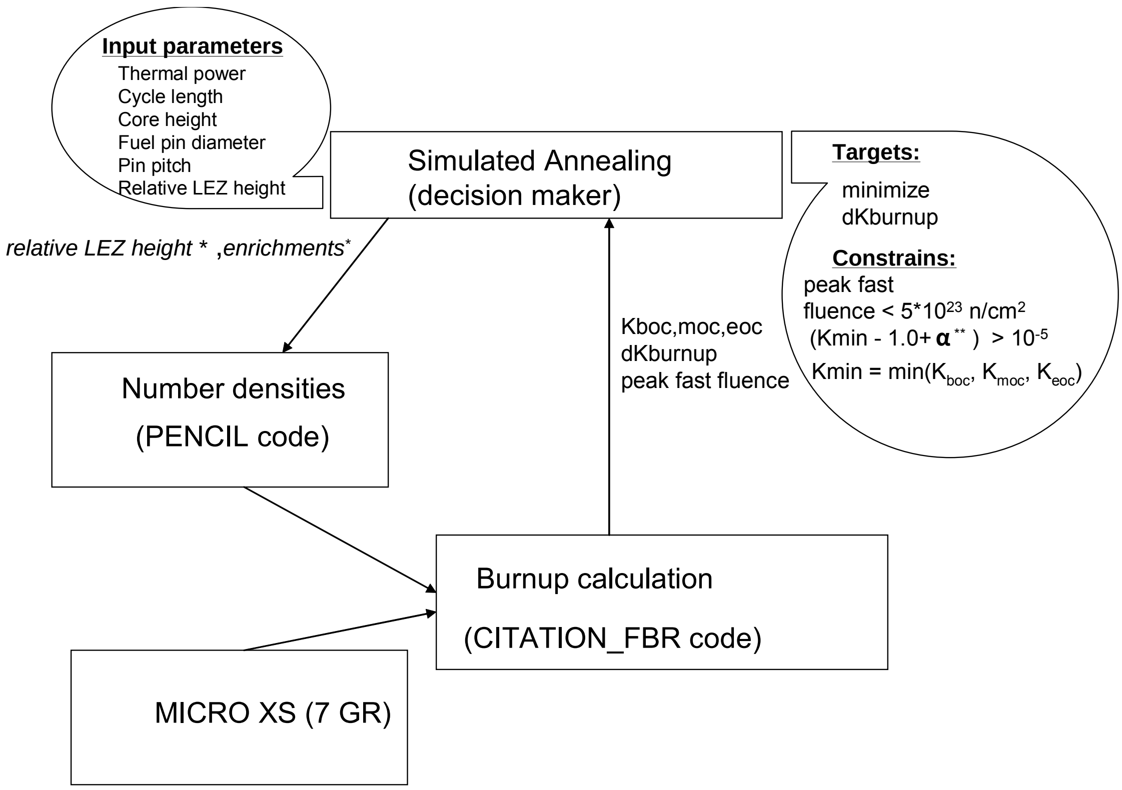

*decision variables
** correction factor (mesh, group, transport)

Fig. 15. Schematics of SAOS calculation optimization system.

SAOS manipulates by inner, outer core enrichments and relative height of axial enrichment heterogeneity, which are selected as decision variables (See Figure 16).

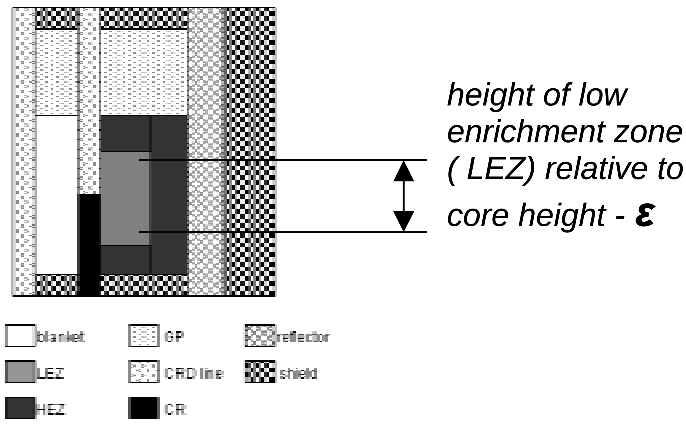

Fig 16. Explanation of decision variable - ε.

3.1.3. Optimization results

As it was mentioned in previous section, the following optimization problem has been considered:

<u>objective</u> – minimization of burnup reactivity swings;

<u>decision variables</u> – enrichments of LEZ , HEZ and value of axial enrichment heterogeneity for inner core region;

<u>constraints</u> – peak fast fluence, minimum value of multiplication factor during core lifetime.

Estimate of minimum value of multiplication factor take into account mesh size, group and transport (leakage) correction factor.

Calculation results are demonstrated by Figures 17-24.

As it seen from Figure 21, the peak fast fluence never exceeded the upper limitation during optimization. Thus, the minimum value of multiplication factor being under lower limitation is the only contributor to penalty function. It is also seen that the optimization problem is almost converged to the near-optimum solution at ~ 1500 evaluations. Simulated Annealing, however, continue “tuning” the near-optimum solution up to ~ 2100 evaluation because of strict convergence criteria being imposed (50 evaluations without improvement of objective function).

As the result of optimization the following solution have been found:

Enrichment of LEZ - 8.0440 % HM;
Enrichment of HEZ - 15.6872 % HM;
LEZ height - 74.75 cm.

These decision variables provides burnup reactivity swings ~ 0.1% during core lifetime of 30 years.

It should be noted that the SAOS system can further be extended with respect to decision variables (core height, fuel pin pitch) and constrains (void reactivity) by modification of evaluation module. Moreover, coupling neutronics with steady-state thermal hydraulics would allow to treat such constrains as maximum coolant velocity, pressure drop, hot spot cladding temperature, etc.

The extension of space of decision variables and increase of time per one evaluation will meet, however, the problem associated with computation costs.

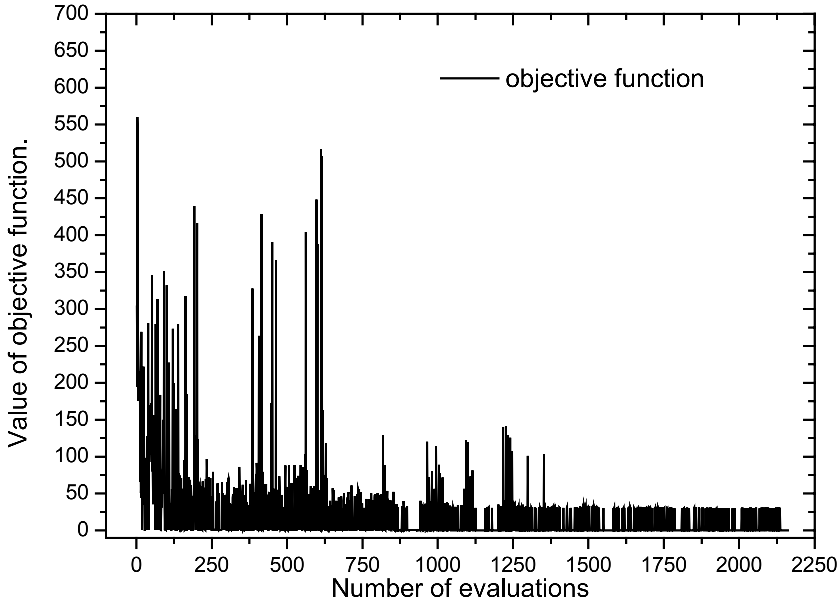

Fig. 17. Objective function.

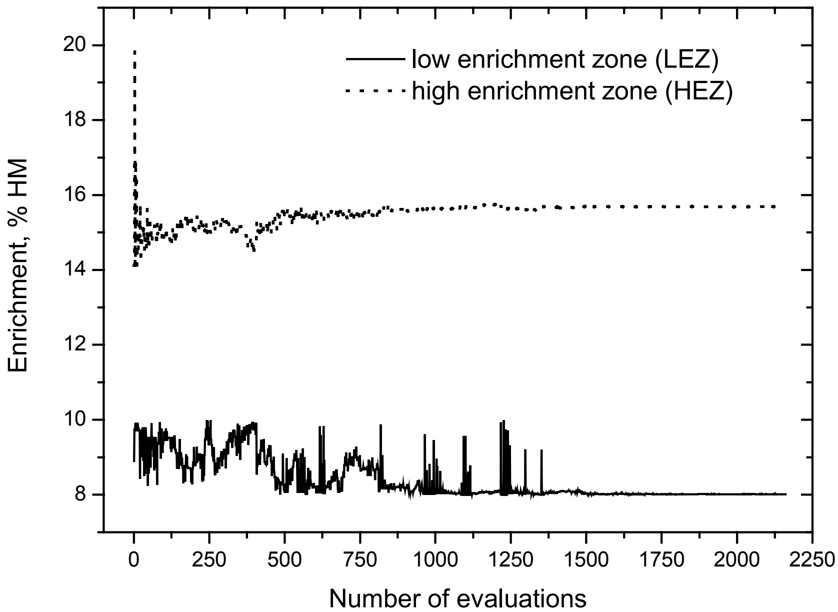

Fig. 18. Enrichments of LEZ and HEZ.

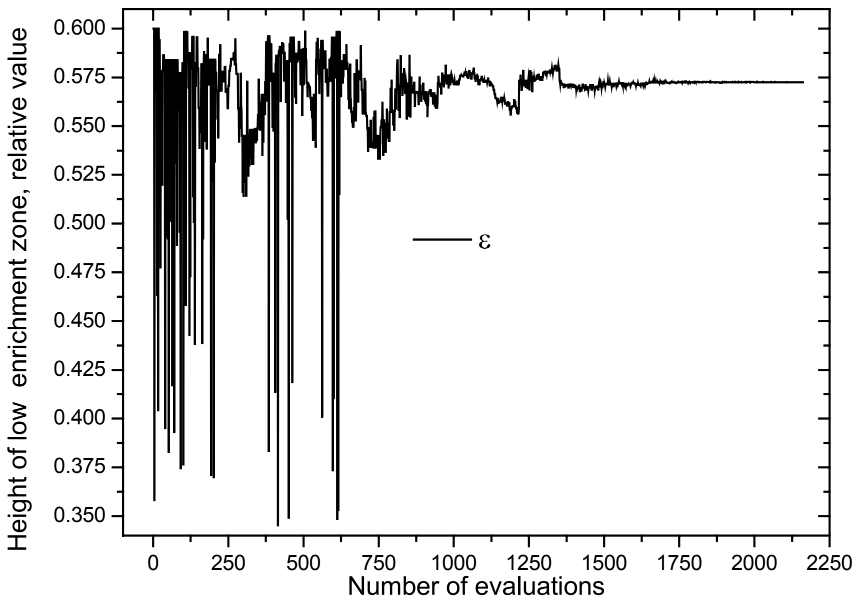

Fig. 19. Relative height of low enrichment zone.

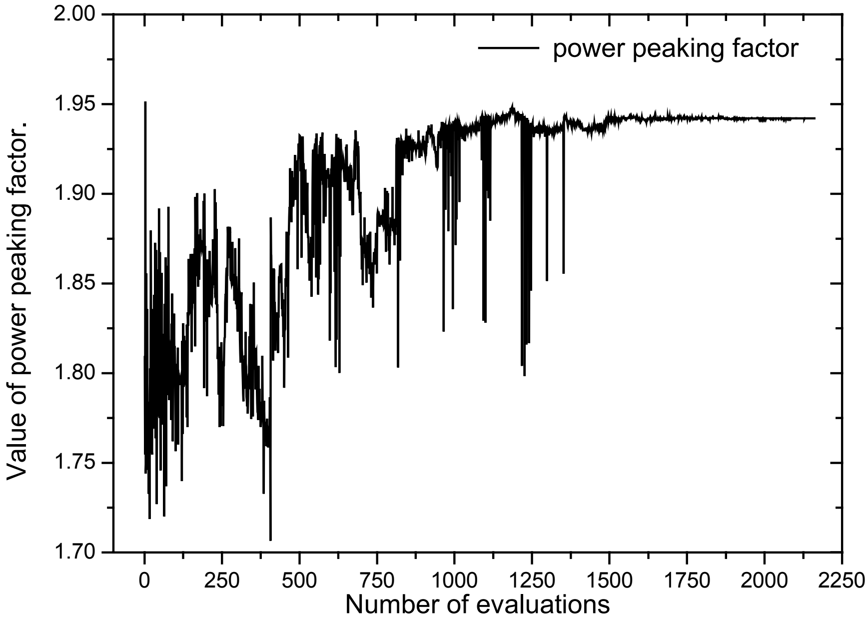

Fig. 20. Value of power peaking factor (maximum during cycle).

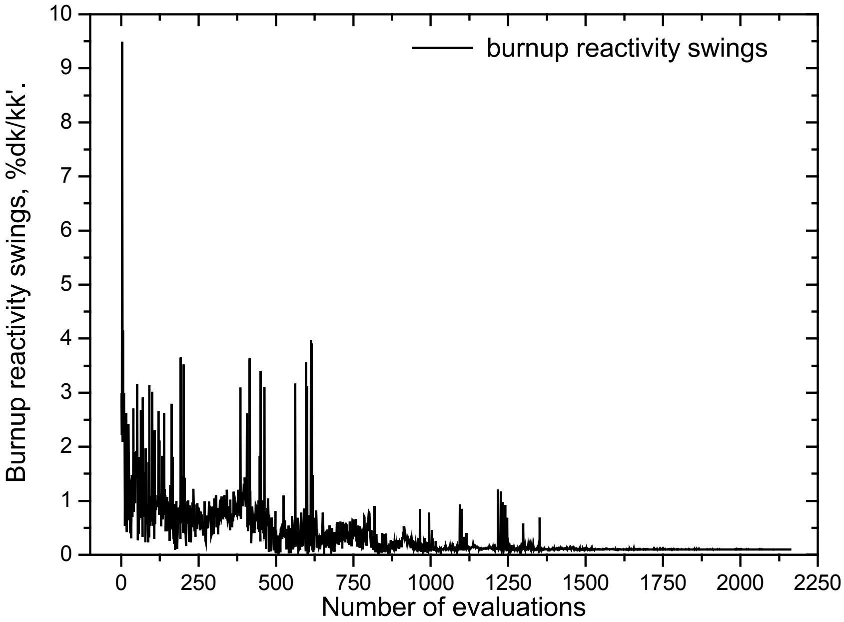

Fig. 21. Value of burnup reactivity swings

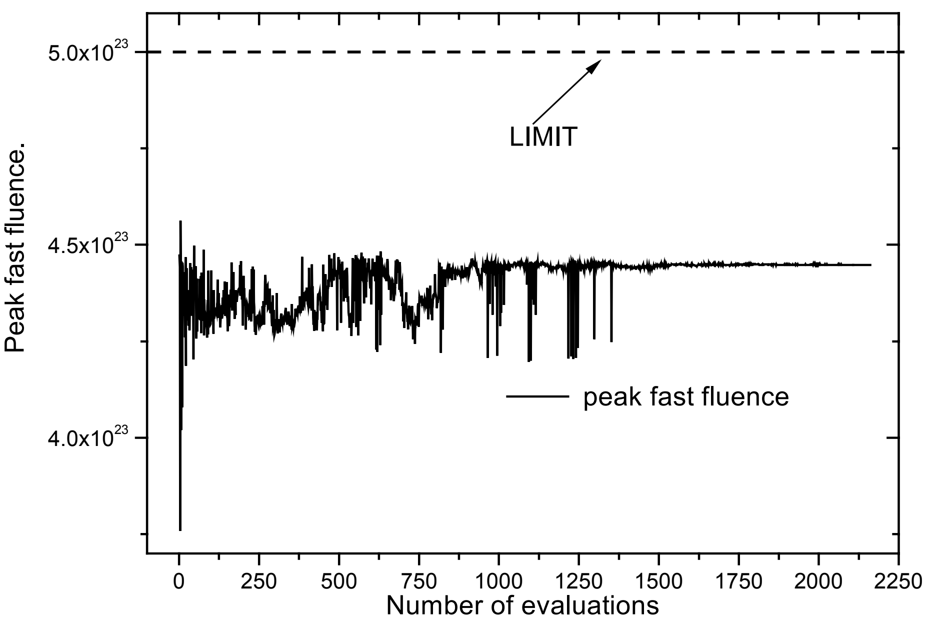

Fig. 22. Value of peak fast fluence

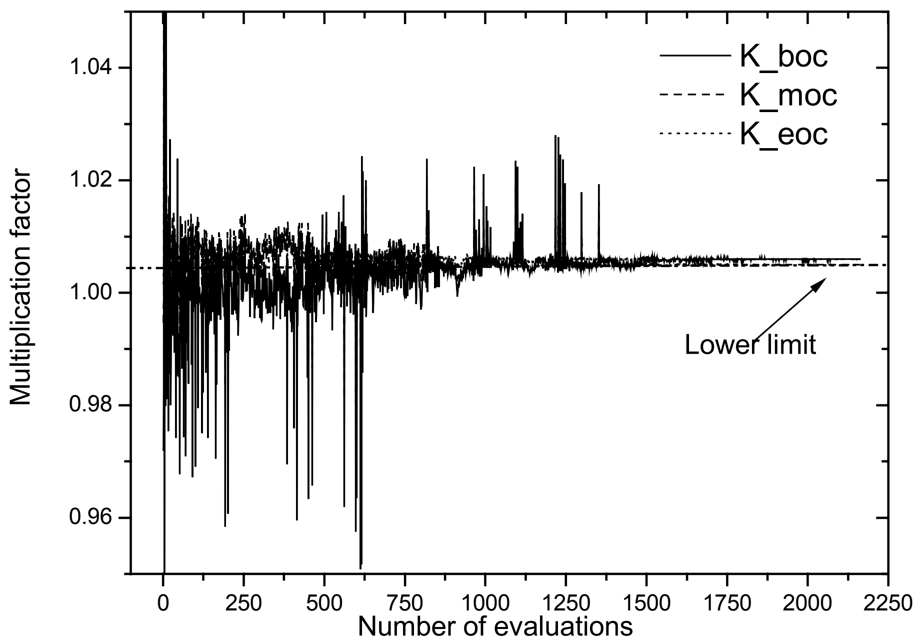

Fig. 23. Multiplication factor.

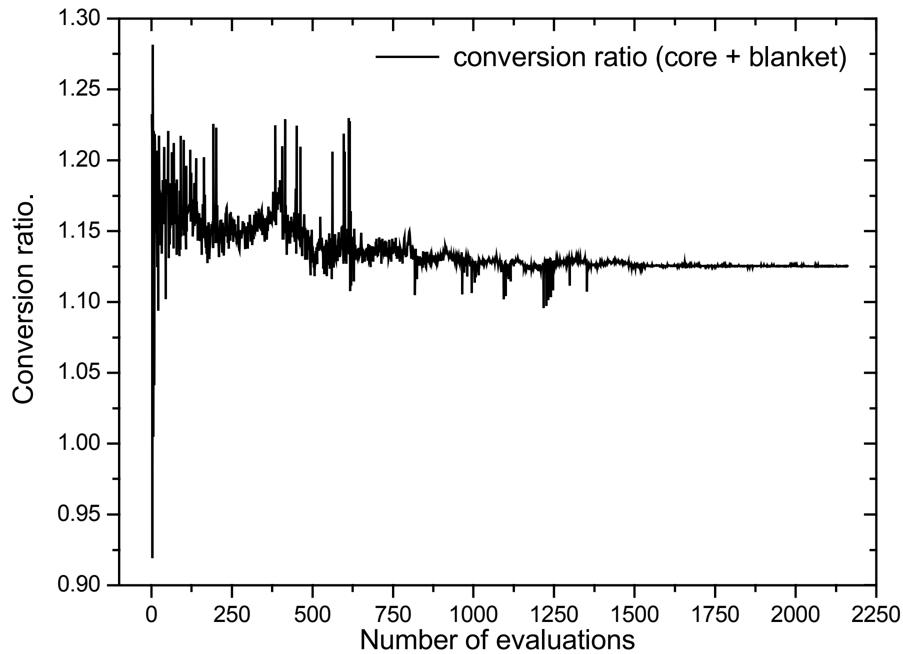

Fig. 24. Value of conversion ratio.

3.2. Specifications and core characteristics of optimized design

Tables10, 11 and 12 demonstrate the reference core specifications, S/A specifications, and optimized core performance, respectively. The core has inner blanket region and axial enrichment heterogeneity in the inner core region. The pitch of fuel in the inner blanket region is the same as in the low and high enrichment zones.

Table 10. Design parameters of optimized core.

Parameter	Value
Thermal output, MWt	150
Core lifetime, years	30
Core equivalent diameter, cm	194.97
Core fuel column length, cm	130.0
Low enrichment zone height, cm	74.75
Top/ Bottom shielding thickness, cm	22.5 / 65.0
Fuel material	(Pu,U) ^{15}N
Clad material	ODS
Wrapper material	PNC-FMS
Coolant material	Pb-Bi eutectic
Bonding material	Pb-Bi eutectic
Core support plate	316FR
CRD line	PNC-FMS
Above core load pads	PNC-FMS
Total number of assemblies	169
S/A pitch, mm	237.73
Number of (core+blanket) assemblies	51+6
Number of reflector assembles	30
Number of shielding assemblies	78
Number of CR assemblies	4
Primary condition (inlet/outlet), C	360/510
Temperature rise	150
Total flow rate, kg/s	6830

Table 11. Fuel subassembly specifications of optimized core.

Parameter	Value
Pin diameter, mm	14 .970
Cladding thickness, mm	0.800
Pellet diameter, mm	**12.250**
Pellet cladding gap, mm	**0.560**
Pin pitch, mm	17.470
Pin gap, mm	2.470
Pitch/diameter ratio	1.165
Total number of fuel pins	9633
S/A size (flat-to-flat), mm	235.73
S/A wall thickness, mm	2.0
Number of fuel pins per S/A	169
Porosity per ring	4.4070
Fuel smeared density, % TD	**84**
Fuel pellet density, % TD	100
Gas plenum length, cm	70.0
CDF (EOC)	(not estimated)
Fuel pin bundle spacing	Grid spacers

Table 12. Performance of optimized core.

Parameter		Value
Average linear power rating , W/cm		119.8
Maximum linear power rating, W/cm	[EOC]	233.0
Peak power factor	[EOC]	1.945
Conversion ratio	[MOC]	1.125
Peak fast neutron dose (E > 0.1 MeV) n/cm2		4.48e+23
Pu Enrichment (inner/outer core), %		8.0440/ 15.6872
Burnup reactivity swings, dk/(kk')%		0.10
HM inventory, kg		19867.76
Average burnup , GWd/t		82.67
Peak burnup , GWd/t		160.8
Void (core region), dk/(kk')%, [$]		2.485E-2, [7.24]

Table 13. Reactivity coefficients distribution (Doppler) (Opt. core).

Ch 1	Ch 2	Ch 3	Ch 4	Ch 5	Ch 6	Ch 7
0.000E+00	0.000E+00	0.000E+00	0.000E+00	0.000E+00	0.000E+00	0.000E+00
0.000E+00	0.000E+00	0.000E+00	0.000E+00	0.000E+00	0.000E+00	0.000E+00
0.000E+00	-8.248E-05	0.000E+00	-2.050E-04	-1.937E-04	0.000E+00	0.000E+00
0.000E+00	-3.671E-05	0.000E+00	-9.322E-05	-9.194E-05	0.000E+00	0.000E+00
0.000E+00	-3.517E-05	0.000E+00	-9.437E-05	-9.542E-05	0.000E+00	0.000E+00
0.000E+00	-2.919E-05	0.000E+00	-8.904E-05	-9.187E-05	0.000E+00	0.000E+00
0.000E+00	-2.047E-05	0.000E+00	-7.807E-05	-8.122E-05	0.000E+00	0.000E+00
0.000E+00	-1.952E-05	0.000E+00	-1.148E-04	-1.192E-04	0.000E+00	0.000E+00
0.000E+00	0.000E+00	0.000E+00	0.000E+00	0.000E+00	0.000E+00	0.000E+00
TOTAL CORE		dK/KK'	: -1.571E-03			

Table 14. Reactivity coefficients distribution (fuel density) (Opt. core).

Ch 1	Ch 2	Ch 3	Ch 4	Ch 5	Ch 6	Ch 7
0.000E+00	0.000E+00	0.000E+00	0.000E+00	0.000E+00	0.000E+00	0.000E+00
0.000E+00	0.000E+00	0.000E+00	0.000E+00	0.000E+00	0.000E+00	0.000E+00
0.000E+00	2.073E-03	0.000E+00	4.124E-02	3.684E-02	0.000E+00	0.000E+00
0.000E+00	1.357E-03	0.000E+00	1.929E-02	1.885E-02	0.000E+00	0.000E+00
0.000E+00	1.082E-03	0.000E+00	1.931E-02	1.922E-02	0.000E+00	0.000E+00
0.000E+00	5.345E-04	0.000E+00	1.784E-02	1.786E-02	0.000E+00	0.000E+00
0.000E+00	2.014E-04	0.000E+00	1.493E-02	1.500E-02	0.000E+00	0.000E+00
0.000E+00	-1.129E-04	0.000E+00	2.158E-02	2.152E-02	0.000E+00	0.000E+00
0.000E+00	0.000E+00	0.000E+00	0.000E+00	0.000E+00	0.000E+00	0.000E+00
TOTAL CORE		(dK/KK')/(dρ/ρ): 2.686E-01				

Table 15. Reactivity coefficients distribution (structure density) (Opt. core).

Ch 1	Ch 2	Ch 3	Ch 4	Ch 5	Ch 6	Ch 7
0.000E+00	0.000E+00	0.000E+00	0.000E+00	0.000E+00	0.000E+00	0.000E+00
0.000E+00	0.000E+00	0.000E+00	0.000E+00	0.000E+00	0.000E+00	0.000E+00
0.000E+00	-6.607E-05	0.000E+00	-6.030E-03	-3.749E-03	0.000E+00	0.000E+00
0.000E+00	-1.656E-04	0.000E+00	-3.961E-03	-2.600E-03	0.000E+00	0.000E+00
0.000E+00	-3.315E-04	0.000E+00	-3.903E-03	-2.700E-03	0.000E+00	0.000E+00
0.000E+00	-5.150E-04	0.000E+00	-3.310E-03	-2.446E-03	0.000E+00	0.000E+00
0.000E+00	-5.981E-04	0.000E+00	-2.452E-03	-1.913E-03	0.000E+00	0.000E+00
0.000E+00	-1.079E-03	0.000E+00	-1.969E-03	-1.559E-03	0.000E+00	0.000E+00
0.000E+00	0.000E+00	0.000E+00	0.000E+00	0.000E+00	0.000E+00	0.000E+00
TOTAL CORE				(dK/KK')/(dρ/ρ):	-3.779E-02	

Table 16. Reactivity coefficients distribution (coolant density) (Opt. core).

Ch 1	Ch 2	Ch 3	Ch 4	Ch 5	Ch 6	Ch 7
0.000E+00	0.000E+00	0.000E+00	0.000E+00	0 .000E+00	0.000E+00	0.000E+00
0.000E+00	2.071E-04	0.000E+00	3.219E-03	5.052E-03	**2.110E-03**	0.000E+00
0.000E+00	-7.492E-04	0.000E+00	-4.323E-03	-1.342E-03	**8.826E-03**	0.000E+00
0.000E+00	-4.878E-04	0.000E+00	-3.602E-03	-1.645E-03	**4.091E-03**	0.000E+00
0.000E+00	-3.824E-04	0.000E+00	-3.491E-03	-1.730E-03	**3.478E-03**	0.000E+00
0.000E+00	-1.685E-04	0.000E+00	-2.822E-03	-1.537E-03	**2.583E-03**	0.000E+00
0.000E+00	-7.063E-06	0.000E+00	-1.947E-03	-1.117E-03	**1.634E-03**	0.000E+00
0.000E+00	1.716E-04	0.000E+00	-4.420E-04	1.695E-04	**1.596E-03**	0.000E+00
0.000E+00	0.000E+00	0.000E+00	0.000E+00	0.000E+00	0.000E+00	0.000E+00
CORE			(dK/KK')/ (dρ/ρ):	-2.324E-02		
GAS PLENUM			(dK/KK')/ (dρ/ρ):	8.361E-03		
RADIAL REFLECTOR			(dK/KK')/ (dρ/ρ):	**2.432E-02**		

Table 17. Delayed neutron data for optimized design (Opt. core).

Parameter	Value
Prompt neutron lifetime	2.51868E-7
Delayed neutron fraction	3.38434E-3
β1	7.22028E-5
β2	7.41962E-4
β3	6.32398E-4
β4	1.26809E-3
β5	5.69830E-4
β6	2.13455E-4
λ1	1.30205E-2
λ2	3.13579E-2
λ3	1.34443E-1
λ4	3.45093E-1
λ5	1.36442E+0
λ6	3.71823E+0

3.3. Verification of load following capability for optimized core

Since modifications made to reference design increases positive coolant density reactivity (pitch in blanket region is increased) and reduction of Doppler (burnup is increased), the load following capability by feedbacks needs confirmation for the new design. Thus, the transient was recalculated. The calculation results are shown by Figures 25 and 26. Figure 26 demonstrates stable decrease of cladding hot spot temperature during load reduction and confirms feasibility of load following capability without operation of the reactor control system for the optimized design in the frame of described simulation model.

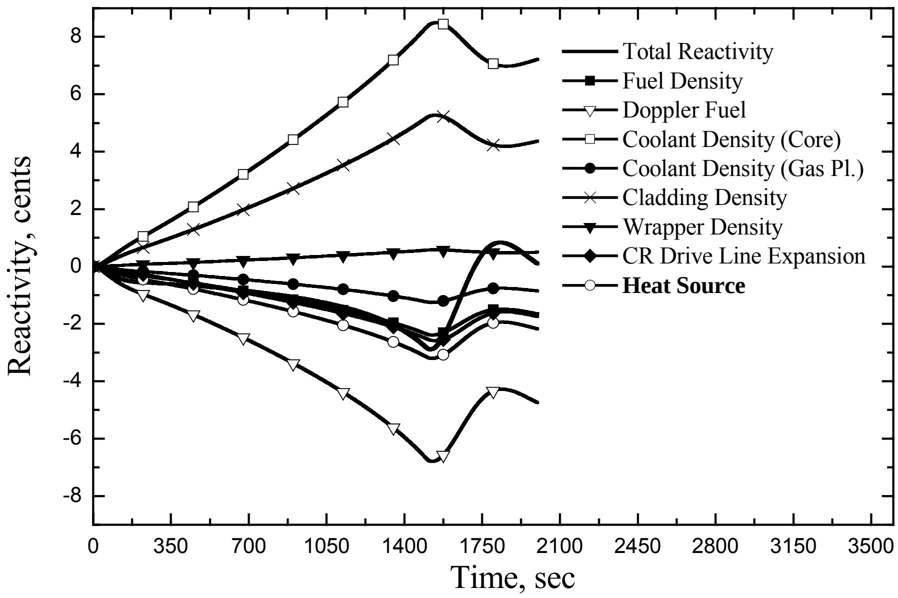

Fig. 25 Reactivity components.

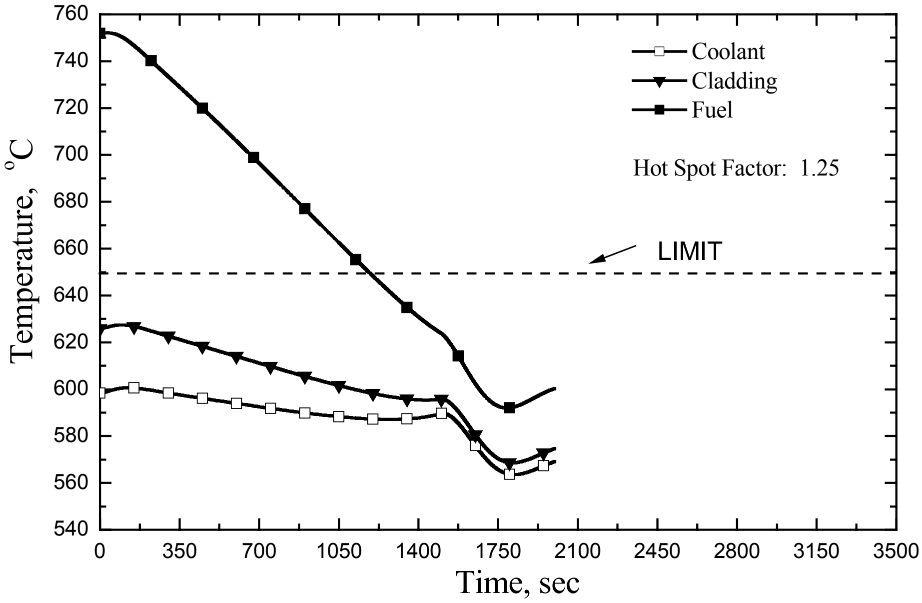

Fig. 26 Hot spot temperatures.

4. CONCLUSION

The load-following capabilities without operation of reactor control system have been investigated for LSPR design, which was taken as reference. It was found that original LSPR design possesses such the feature without violation of the design constraint – the cladding hot spot temperature.

Additionally, the innovation for the reference design has been proposed in order to enhance such the capability. The point of innovation is strengthening of negative reactivity feedback by introduction of heat source (in the form of short fuel pins) at the bottom of radial lead-bismuth reflector. Implementation of the heat source allows controlling radial leakage during load change. In the case of small reactor the radial leakage plays essential role in neutron balance and, thus, utilization of heat source is effective.

At the initial stage, research was performed using simple computational models from neutronics viewpoint (RZ, Diffusion approximation). In order to make the analysis accurate with reasonable requirement on computation costs, several computational approximations were implemented and the best suited for this particular problem had been selected (3D, Diffusion, 18 gr. - for the fuel and structure density reactivity feedbacks; 3D, Transport, 18 gr. – for the coolant density feedbacks).

As the final step of the research, the optimization of reference design have been performed with the purpose to make it simpler (keeping the same fuel pin pitch for all core) and economically competitive (increase of fuel burnup) The load following capability has then been confirmed for optimized design in the frame of described simulation model.

5. ACKNOWLEDGEMENTS

The author is very thankful to:

Mr. Tomoyasu Mizuno and Mr. Naoyuki Takaki for the guidance during this study;

Mr. Hideyuki Hayashi, whose idea of utilization of heat source in radial reflector region, is one of the key findings of that research;

Mr. Hiroshi Endo for helpful advice during development of SPAKS system;

all members of Fuel and Core System Engineering Group for technical suggestions and discussions;

Mr. Hiroshi Komoda for providing excellent computational environment;

Mr. Makoto Ishikawa and several members of NESI Corporation (Mr. Soga, Mr. Iwai, Mr. Sato, Mr. Numata, Mr. Hosono) for their valuable help during mastering neutronics analytical tools.

REFERENCES

1. Toshinsky V., Hayashi H. "Feasibility Study on Small Long-Life PB-BI Cooled Reactor with Capability of Load Following by Flow Rate Adjustment", *Int. Conf. On the New Frontiers of Nuclear Tech.: React. Phys., Safety and High Performance Computing* (PHYSOR2002), October 7-10, 2002, Seoul, Korea, (2002).

2. N. Ueda, Y. Nishi, H. Matsumiya and T. Yokoyama, “Passive Reactor Dynamics and Load Following Characteristics of Sodium Cooled Super-Safe Small and Simple Reactor”, *11th International Conference of Nuclear Engineering*, Tokyo, JAPAN, April 20-23,ICONE11-36539 (2003)

3. Zaki Su’id and Hiroshi Sekimoto, “Design and Safety Aspect of Lead and Lead-Bismuth Cooled Long-Life Small Safe Fast Reactors for Various Core Configurations ”, *Journal of Nuclear Science and Technology,* 32[9], pp. 834-845 (1995)

4. H.Sekimoto, S.Makino, K.Nakamura, Y.Kamishima, and T.Kawakita “Long-Life Small Reactor for Developing Countries, LSPR”, *Int. Seminar on Status and Prospects for Small and Medium Sized Reactors,* Cairo, Egypt ,27-31 May (2001).

5. “Brief report on the research by JNC Postdoctoral Fellows for 2002”, pp. 52-63 JNC TN1400 2003-009 (2003).

6. S. Hunter “Fast Reactor Calculational Route for Pu Burning Core Design”, PNC TN9460 98-001.

7. Toshinsky V., Hayashi H. "Enhancement of Reactivity Feedback at ULOF for Small Size Long-Life Pb-Bi Cooled Reactor by Implementing Heat Source in Radial Reflector", *Trans. Int. Youth Nuclear Congress* (IYNC2002), p.158, April 16-20, 2002, Taejon, Korea, (2002).